SAND2014-20243C

Development and Assessment of Advanced Inspection Methods for Wind Turbine Blades Using a Focused WINDIE Experiment

Dennis Roach[1], Stephen Neidigk[2], Tom Rice[2], Randy Duvall[3], Josh Paquette[4]
Sandia National Labs
Albuquerque, NM 87185 U.S.A.

Wind turbine blades pose a unique set of inspection challenges that span from very thick and attentive spar cap structures to porous bond lines, varying core material and a multitude of manufacturing defects of interest. The need for viable, accurate nondestructive inspection (NDI) technology becomes more important as the cost per blade, and lost revenue from downtime, grows. NDI methods must not only be able to contend with the challenges associated with inspecting extremely thick composite laminates and subsurface bond lines but must also address new inspection requirements stemming from the growing understanding of blade structural aging phenomena. Under its Blade Reliability Collaborative program, Sandia Labs quantitatively assessed the performance of a wide range of NDI methods that are candidates for wind blade inspections. Custom wind turbine blade test specimens, containing engineered defects, were used to determine critical aspects of NDI performance including sensitivity, accuracy, repeatability, speed of inspection coverage, and ease of equipment deployment. The Sandia Wind NDI Experiment (WINDIE) was completed to evaluate fifteen different NDI methods that have demonstrated promise for interrogating wind blades for manufacturing flaws or in-service damage. These tests provided the information needed to identify the applicability and limitations of advanced inspection methods for wind turbine blades. Ultimately, the proper combination of several inspections methods may be required to produce the best inspection sensitivity and reliability for both near-surface and deep, subsurface damage. Based on these results, phased array ultrasonics was selected for further development and introduction at blade manufacturing facilities. Hardware was developed and customized to optimize UT sensitivity and deployment to address blade inspection needs. Inspection procedures were produced and beta tested at blade production facilities. This study has identified one optimum overall NDI method while determining complimentary NDI methods that can be applied to produce a comprehensive blade inspection system. The detection of fabrication defects helps enhance plant reliability and increase blade life while improved inspection of operating blades can result in efficient blade maintenance, facilitate repairs before critical damage levels are reached and minimize turbine downtime.

I. Wind Inspection NDI Experiment (WINDIE)

The development and deployment of advanced nondestructive inspection (NDI) methods must keep pace with the rapidly-increasing size and complexity of modern wind turbine blades. Nondestructive inspection requirements, methods and practices vary widely within the wind industry. Different blade manufacturers utilize different levels of rigor and different inspection methods on their product before it leaves the factory. As the length of blades increase and more advanced materials are being used to manufacture blades, it has become increasingly important to detect fabrication defects during blade production, thus enhancing plant reliability.

[1] Senior Scientist, Transportation Safeguards and Surety org., PO Box 5800 MS-0615
[2] Staff Member, Infrastructure Surety and NDI Dept., PO Box 5800 MS-0615
[3] Technologist, Infrastructure Surety and NDI Dept., PO Box 5800 MS-0615
[4] Staff Member, Wind Energy Technologies Dept., PO Box 5800 MS-1124

The purpose of the Wind Inspection NDI Experiment (WINDIE) was to determine the capability of conventional and advanced Nondestructive Inspection (NDI) methods to identify flaws in wind turbine blades. The WINDIE effort was used to study the capabilities and limitations of numerous NDI methods in identifying the different flaw types in wind blade construction. The general goal was to determine which NDI method(s) have high sensitivity, accuracy and reliability in order to identify those with promise for continued development and application. This effort also identified the factors influencing composite wind blade inspections on this type of structure so that improved methods and procedures can be developed.

The test specimens used to evaluate the maturity and viability of a wide range of NDI methods contained an array of different, representative flaw types and wind turbine blade construction types. Engineered test specimens and damaged wind blade sections acquired from the field were used to establish the ability of advanced NDI methods to detect manufacturing flaws and in-service damage including: snowflaking, voids, interply delaminations, resin-starved regions, spar and shear web disbonds, ply waviness, adhesive voids, fiber fracture, erosion, impact, lightning strike, and fluid ingress. Figures 1 and 2 show sample flaw types and test specimen drawings. The NDI specimens were applied in a "feedback" mode where the inspector was aware of the flaw profile in each specimen (i.e. not blind mode inspections). Each experimenter was provided with drawings of each specimen type which showed the structural configuration as well as the definition and location of each flaw. They were asked to inspect each specimen/blade section and provide any information about the presence of flaws. If they determined that the flaws are detectable, they captured the required inspection data to provide some type of signal or image showing the flaw(s). The results were compiled in a structured manner to arrive at preliminary rankings of performance.

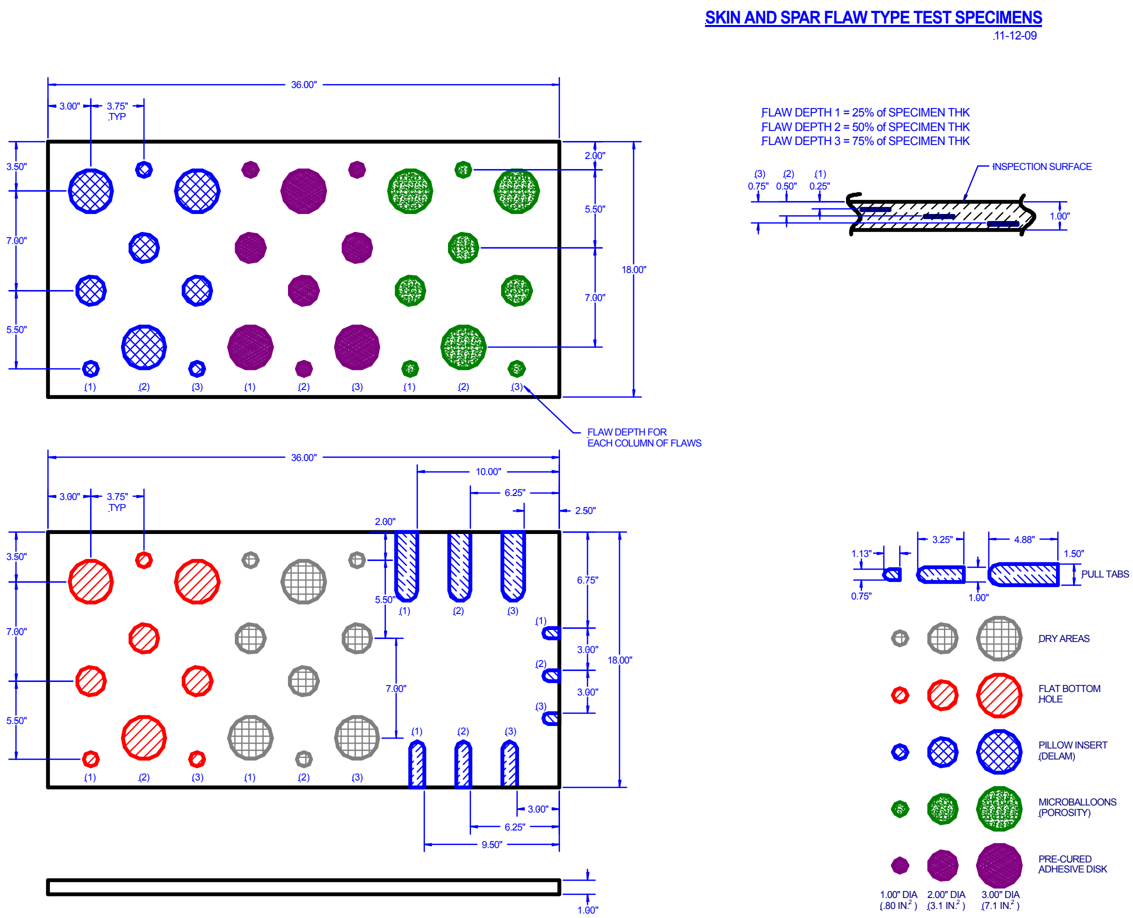

Figure 1. Skin and Spar Test Specimen Drawing.

Candidate NDI methods included: Through Transmission Ultrasonics (TTU), Pulse-Echo UT, Pulse-Echo UT with Focused Probe, Phased Array UT, UT Spectroscopy, Resonance, Thermography (flash, locked-in, inductance, line, Sonic IR), Microwave, Mechanical Impedance Analysis, Low Frequency Bond Test, Shearography and quantitative interferometric measurements (e.g. 3-D strain mapping), Terahertz, Digital Radiography, Backscatter X-ray, and Laminography. Table 1 provides the list of NDI methods and potential participants that were identified for inspection of wind blades. The check marks indicate the resulting set of WINDIE participants and the associated set of NDI methods that were actually applied to the NDI test specimens.

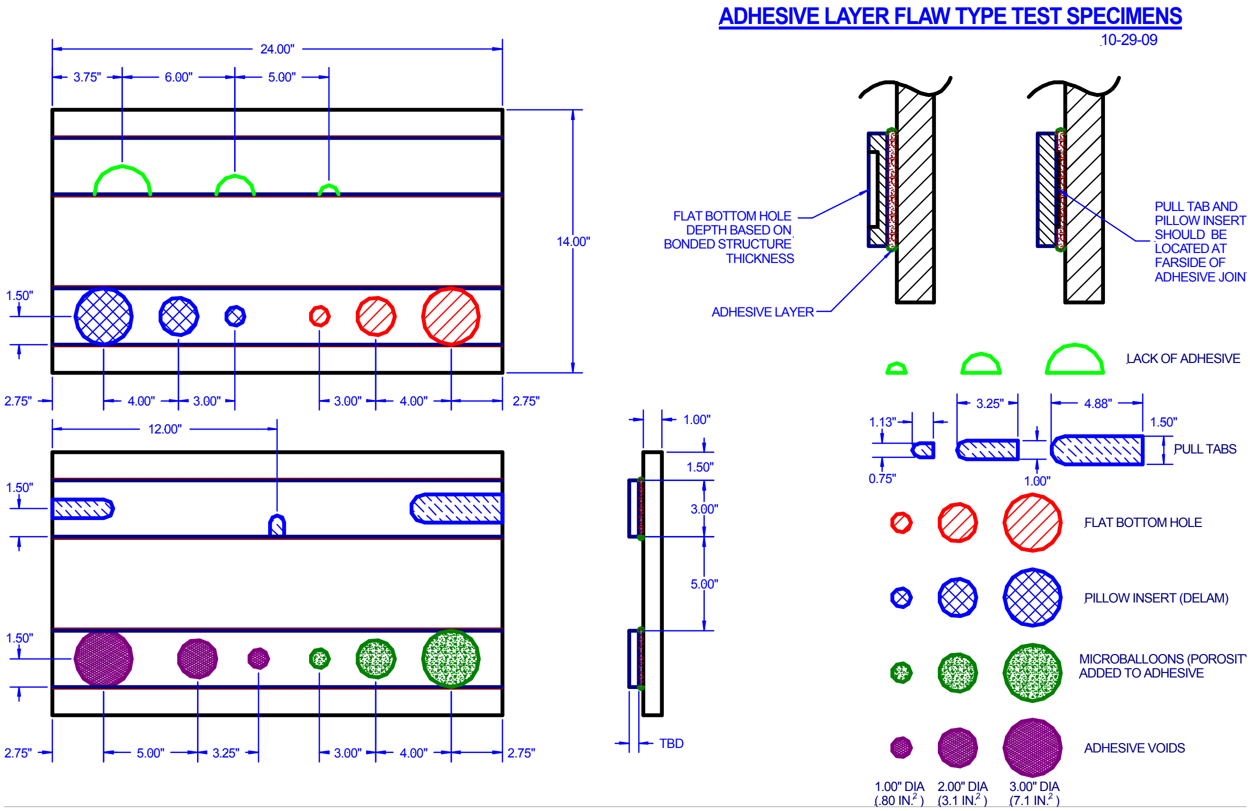

Figure 2. Adhesive Layer Test Specimen Drawing.

The experiment tasks involved in this round-robin testing program were: 1) fabrication of representative test specimens to be used with all inspection methods, 2) comprehensive, in-house characterization of the NDI test specimens to ensure flaw realism, 3) production of experiment protocols, NDI candidate list, and invitation to possible participants, 4) completion of round-robin testing on NDI test specimens with a wide range of NDI methods, and 5) completion of analysis of inspection results with NDI comparisons (sensitivity, repeatability, coverage, adaptability deployment, cost, etc.). Other information gathered during round-robin inspections included: a) duration of inspection, b) fieldability (portable), c) deployment issues, d) inspection method difficulties, e) cost of new system, f) accessories needed to make the inspection device fieldable, g) ease of data interpretation.

	Inspection Method	Company
✓	Linear Array UT 3D Matrix Eye	Toshiba
✓	Phased Array UT	Olympus NDT
	Acoustic Emission	iHMSi
✓	Air Coupled UT	ISU
	ANDSCAN-Robot	Genesis Systems
	Bandicoot	CSIRO
	Custom Systems	Exova
✓	Digital Acoustic Video (Acoustacam)	Imperium
	Digital Image Correlation (DIC)	Dantec Dynamics
	Flaw Inspecta UT Array	NDT Solutions Inc
✓	Focused Probe Immersion UT	GE Inspection Technologies
	Guided Ultrasonics	Guided Ultrasonics
✓	Induction Thermography System & Air Coupled UT	Boeing
	Induction Thermography System (ITS)	Quest Integrated Inc
✓	IR Inspection Ssytem (IRIS)	Vista Engineering Technologies
	Laminography	Digiray
✓	Laser UT	iPhoton
	Line Thermography	Mistras Group
	Linear Array UT	USUT Labs/Veracity
✓	Lock-In Thermography	moviMED/MoviTherm
	MAUS MIA Mode	AANC
	MAUS Resonance Mode	AANC
✓	Microwave	GE Global Research
✓	Microwave NDE	Evisive
✓	Millimeter Wave Inspection Tool	Physical Optics Corp. (POC)
✓	Phased Array UT	AANC
	Pulse Echo UT	QinetiQ
✓	RapidScan2 (Phased Array Wheel Probe)	Sonatest/R-CON NDT
	Rotor Blade CT System	iHMSi
✓	Shearography	Dantec Dynamics
	Shearography	Laser Technology Inc
	Sonic IR	WSU
	Terahertz	Teraview
✓	Terahertz Radiation (T-Ray)	Iowa State University
	Terrahertz Imaging	GMA Industries
	Thermography	AANC
✓	Thermography	Thermal Wave Imaging
✓	Through Transmission	AANC
	Ties to QinetiQ	Triton Systems
✓	TSCOUT (Thick Section Comp. UT) & PAC UT	Mistras Group
	UT and IR Systems	TecScan
	UT Spectroscopy	QinetiQ
	Various NDI	IHI Southwest Technologies
✓	Vibro Thermography	Resodyne
✓	MAUS Phased Array UT	AANC
✓	RotoArray - Phased Array UT	GE Inspection Technologies

Table 1. Candidate Participants in the Sandia Labs WINDIE Experiment.

II. Results from WINDIE Experiment

It is not possible to present all of the results from each advanced NDI method that participated in the WINDIE experiment. A set of results will be presented for select NDI methods, including the top performer and some methods that provide niche inspection capabilities, in order to provide an overview of the type of results obtained. The following sections are broken down into the set of inspection results NDI method selected. The comprehensive set of results can be found in Reference 1.

A. Microwave Technique

The sensitivity level of microwave radar depends on several factors including power of the transmitter, frequency range and directional selectivity of the antenna. Flaws are inferred by changes in the dielectric constant. The major benefit to microwave inspection technology is that it is a non-contact method of inspection. There is no coupling media required to inspect the part, eliminating the need for surface contouring that uses custom contact deployment hardware. However, a gantry system or scanning method would need to be developed for field and factory use. Microwave systems typically inspect with a frequency sweep across the range of 1-20 GHz. This is followed by the application of a Fast Fourier Transform to the data to produce A, B, and C scans. The scan head is placed approximately 0.2 m from the front of the part to be inspected.

While the Evisive Scan microwave inspection method had not been optimized for the WINDIE parts, the scan results do give the viewer an idea of the capabilities of the system on wind turbine blade sections. The images presented were created by the two separate hardware channels of the Evisive Scan transducer, each with two possible frequencies. A single scan was performed for each frequency. The two different frequencies differ in phase and hence differ in the depth at which the image is optimized.

Each wind part was scanned using the Evisive microwave imaging equipment. It can be seen in some of the results that the Evisive Scan system can detect and image unintentional defects in addition to the intentionally placed engineered flaws. In order to mark a flaw as detected, the scan image was reviewed and locations of areas where the return signal (voltage) differed from the general return signal for the part were identified. Indications were correlated to a possible cause based on previous experience with fiberglass inspections. Preliminary set up on calibration curves allowed the depth of the flat bottom holes to be measured. The Evisive scanning system with the 24 GHz transducer is shown on the left side of Figure 3. The 24 GHz transducer in the multi-axis gimbal is shown in the right side of this figure. This gimbal allowed it to be used on contoured surfaces.

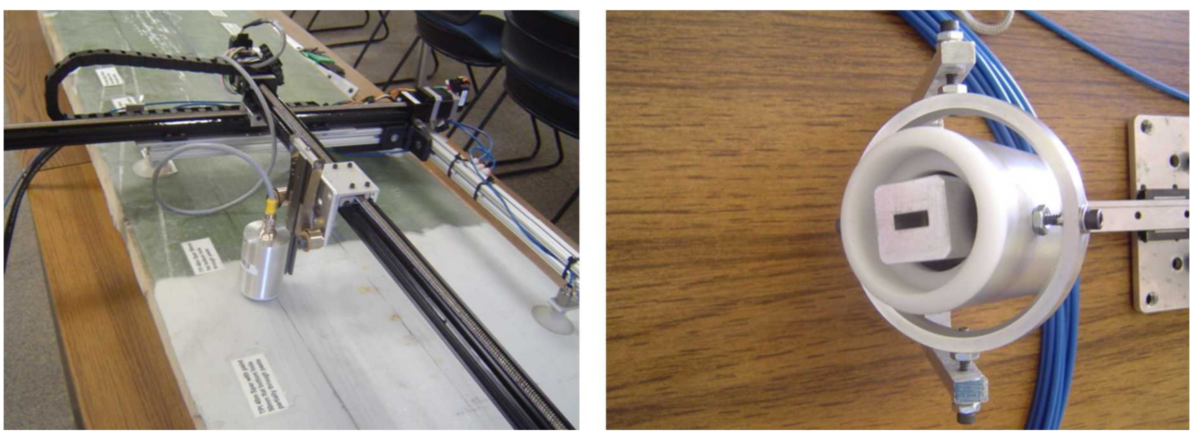

Figure 3. Evisive Microwave Inspection System with 24 GHz Probe.

Overall the 10 GHz probe had a better signal-to-noise ratio than the 24 GHz probe. Also, the 24 GHz probe did not have as much depth of penetration to detect flaws in thicker laminates. The scanning system had a vacuum system that produces active suction cups for attachment to the surface being inspected. Flat bottom holes, pillow inserts, microballoons, out-of-plane waves, and pull tabs were imaged with the Evisive microwave technique in the spar cap laminate. However, the deeper flaws and the flaws in the adhesive bond line beneath the spar cap were more difficult to image and many of these flaws were not detected. The grease and mold release defects were not detected in either the spar cap or the adhesive joint and will need further testing to develop a reliable microwave method for detection. Some probe lift-off issues were identified during the testing due to rough contours on the edges of some specimens. This made flaw calls difficult on some of the specimen edges.

Voltage signals taken on an unflawed and flawed region of a WINDIE specimen can be seen in Figure 4. These signals can be compared to an A-scan signal generated in an ultrasonic inspection and are used to generate the microwave C-scan images. Figure 5 shows the inspection images produce by the Evisive microwave system when inspecting specimen REF-STD-2-127-173-SNL-1. In Figure 5, flat bottom holes in spar cap laminate were detected at the various depths and the flat bottom holes in the bonded shear web joint were also detected. It appears that all sizes of the flat bottom holes were detected (difficult to see 75% FBH – 1.0" diameter in bonded shear web joint). Pull tab flaws in laminate at 25% depth were detected while the deeper pull tab flaws at 75% were not. None of the pull tabs in the shear web bonded joint, both at the upper and lower adhesive interface, were detected.

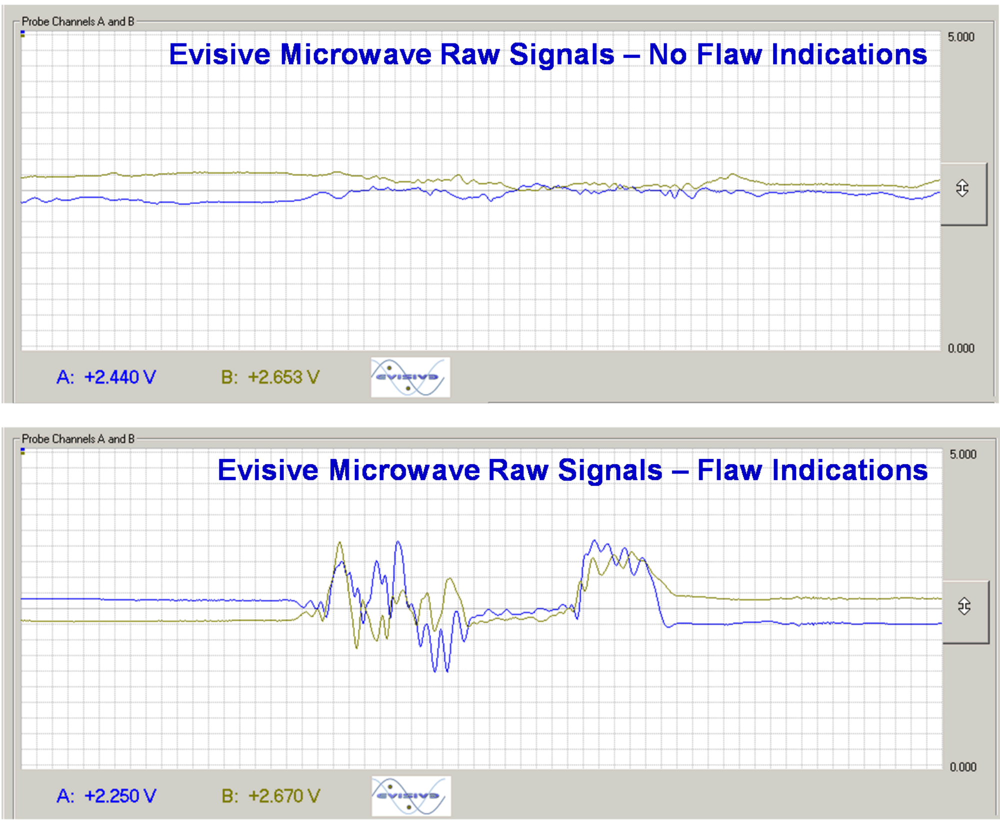

Figure 4. Signals Generated by Evisive Microwave Inspection System Showing the Difference Between Flawed and Unflawed Regions.

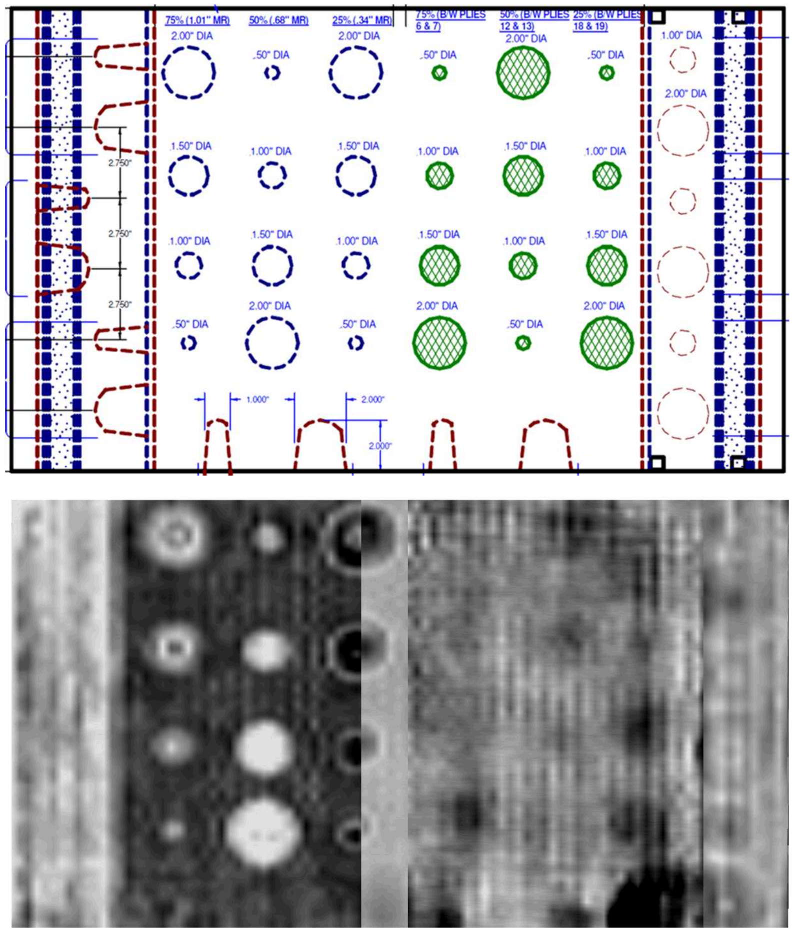

Figure 5. Evisive 24 GHz Microwave Scan of REF-STD-2-127-173-SNL-1 With Spar Cap and Shear Web Bond Line Flaws.

Figure 6 shows microwave results for specimen Wind-2-044-SPAR-085. This specimen represents thin and thick spar caps and include the adhesive joint at the spar cap-to-shear web flange interface. It can be seen that most of the flat bottom holes are detected in the microwave images with the exception of the most challenging flaws that are located on the back side of the adhesive bond line. These flaws are further away from the inspection surface and are very close to the back wall surface making it difficult to image the very small difference in wave travel.

Conclusions on the Microwave inspection method are: 1) the Microwave inspection method can be used on glass reinforced composite components to detect some defects and internal structure, 2) defects are detected by detecting changes in electromagnetic properties or the location of changes in such properties (as in a part surface), 3) the lower frequency 10 GHz probe had a favorable signal-to-noise ratio over the 24 GHz probe, 4) flat bottom holes, pillow inserts, microballoons, wrinkles, and pull tab damage were imaged with the Microwave technique, 5) grease and mold release defects will need further testing to develop a reliable method for detection, 6) defects of a size comparable to those intentionally introduced in the supplied parts (1" dia.) are detectable, even in the presence of complex structure and significant thicknesses, 7) for parts with a solid laminate thickness of up to 1.5 inches, the preferred interrogation frequency is 24 GHz; for thicker laminates, the preferred frequency is 10 GHz, 8) a standard 24 GHz, 5 Mw transducer was used when inspecting these parts. The resolution of the 10 GHz transducer is slightly diminished, compared to the 24 GHz, but is adequate to detect and size the defects included in these test specimens Transducers with higher power outputs are available, should field inspections require them. Additionally, probes with finer resolution due to smaller beam spots can be deployed.

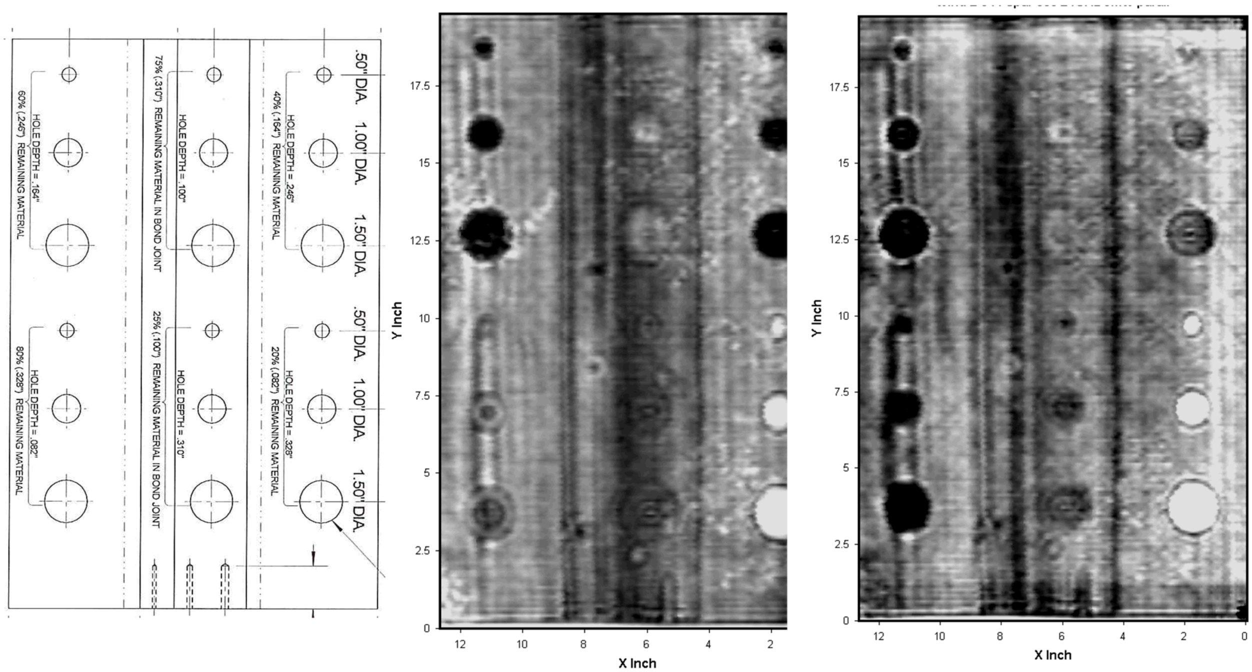

Figure 6. Images of Specimen Wind-2-044-SPAR-085 Showing Evisive Microwave Results for Flat Bottom Hole Flaws in Thin Spar Cap (0.44" th) and Adhesive Shear Web Bond Line (0.85" th.).

B. Phased/Linear Array Ultrasonics

1. Development of Phased Array Ultrasonic System for Wind Blade Inspections

Under its Blade Reliability Collaborative program, Sandia Labs has developed and adapted customized pulse-echo ultrasonic inspection (UT) methods to optimize sensitivity and depth of signal penetration in large wind turbine blades. Specific hardware, system deployment and data analyses approaches were conceived to overcome the unique challenges associated with blade inspections. Some of the key items include optimized inspection frequency, use of focused transducers and focusing apparatus, use of compatible pulser excitations, use of data filters, transducer housing to improve signal coupling, and multiple gate settings to uncouple and identify signals of interest. These innovations optimize signal strength and clarity while allowing the user to focus on key signatures within the blade. This allows for interrogation of both the composite laminate structures and the bond lines below the spar cap and at the trailing edge. Automated and encoded phased array UT inspections were integrated to enable the production of two-dimensional, color coded C-scan images of wide area inspections. This feature improves probability of damage detection, minimizes false calls and improves overall health assessment efforts.

2. Olympus NDT Phased Array Ultrasonic System

Conventional ultrasonic transducers for NDI commonly consist of either a single active element that both generates and receives high frequency sound waves, or two paired elements, one for transmitting and one for receiving. Phased array probes, on the other hand, typically consist of a transducer assembly with 16 to as many as 256 small individual elements that can each be pulsed separately. A phased array system will also include a sophisticated computer-based instrument that is capable of driving the multi-element probe, receiving and digitizing the returning echoes, and plotting that echo information in various formats. Unlike conventional flaw detectors, phased array systems can sweep a sound beam through a range of refracted angles or along a linear path, or dynamically focus at a number of different depths, thus increasing both flexibility and capability in inspection setups.

Phased Array Ultrasonics (PA-UT) involves the use of multiple signals from a contained series of transducers (phased arrays) to produce diagnostic images in the form of ultrasonic C-scans. The operation is similar to hand-held UT, however, the simultaneous use of multiple sensors allows for rapid coverage and two-dimensional images from which to assess structural integrity. Three probe and wedge combinations were used with the majority of the tests performed with the two large aperture combinations. The 25 mm water column (WC) shoe used a contained water column to provide the UT coupling between the probe and the part. The contact wedge used a solid block of an impedance-matching plastic material with a thin film of base water to provide the offset and coupling to the part. The Aqualene wedge used a delay line block made from Aqualene along with a wetted surface to provide the offset and coupling to the part. Figure 7 shows the OmniScan equipment set-up and deployment for these phased array UT inspections.

Figure 7. Phased Array Ultrasonics Inspection with OmniScan System.

Ultrasonic phased array technology, along with the widely adaptable range of probe housings and deployment options were shown to have strong flaw detection capabilities in multiple wind turbine blade structures. These include both thin and thick fiberglass spar cap laminates and bond line interfaces. Near surface flaws (less than 5 mm deep) in thick laminates tend to be more difficult to detect using low frequency ultrasonic techniques due to the dead zone of the probe and high noise levels created at the water path to fiberglass interface. This is caused by the large impedance mismatch between the ultrasonic coupling media (water) and the fiberglass.

Figure 8 shows PA-UT results for specimen Wind Specimen REF-STD-2-127-173-SNL-1. This specimen represents a relatively thick spar cap and includes the adhesive joint at the spar cap-to-shear web flange interface. Insights and summary of results from the OmniScan PA-UT device deployed with the 1.5L42 probe in the 25 mm water column shoe are as follows:

- The 25 mm water column provided good coupling to the specimen and the needed offset (delay line) to avoid the interference of the harmonic signals. Thus, the 25 mm water column allows for inspecting the adhesive joint on this specimen (between the spar and adhesive and between adhesive and shear web).
- This specimen is quite noisy even at 1.5MHz.
- There is a dead-zone of roughly 10 mm near the front surface. This is slightly more than with the contact wedge and may be due to probe backing noise.
- Flat bottom holes in spar cap laminate were detected at the various depths and the flat bottom holes in the bonded shear web joint were also detected. It appears that all sizes of the flat bottom holes were detected (difficult to see 75% FBH – 1.0” diameter in bonded shear web joint). Pull tab flaws in laminate at 25% depth and at 75% depth were detected. The pull tabs in the shear web bonded joint, both at the upper and lower adhesive interface, were detected. Figure 8 shows the amplitude and B-scan (flaw depth) images produced by a back wall gate ranging from 0.4” to 1.6” in depth.
- Back wall gating works well for inspecting the laminate for delamination flaws.
- Alternative gating can be used to specifically look at the adhesive joint.

- Most indications within the laminate showed up relatively well including the 0.50” diameter FBHs and pillow inserts, especially when gating the off of the back wall of the laminate.

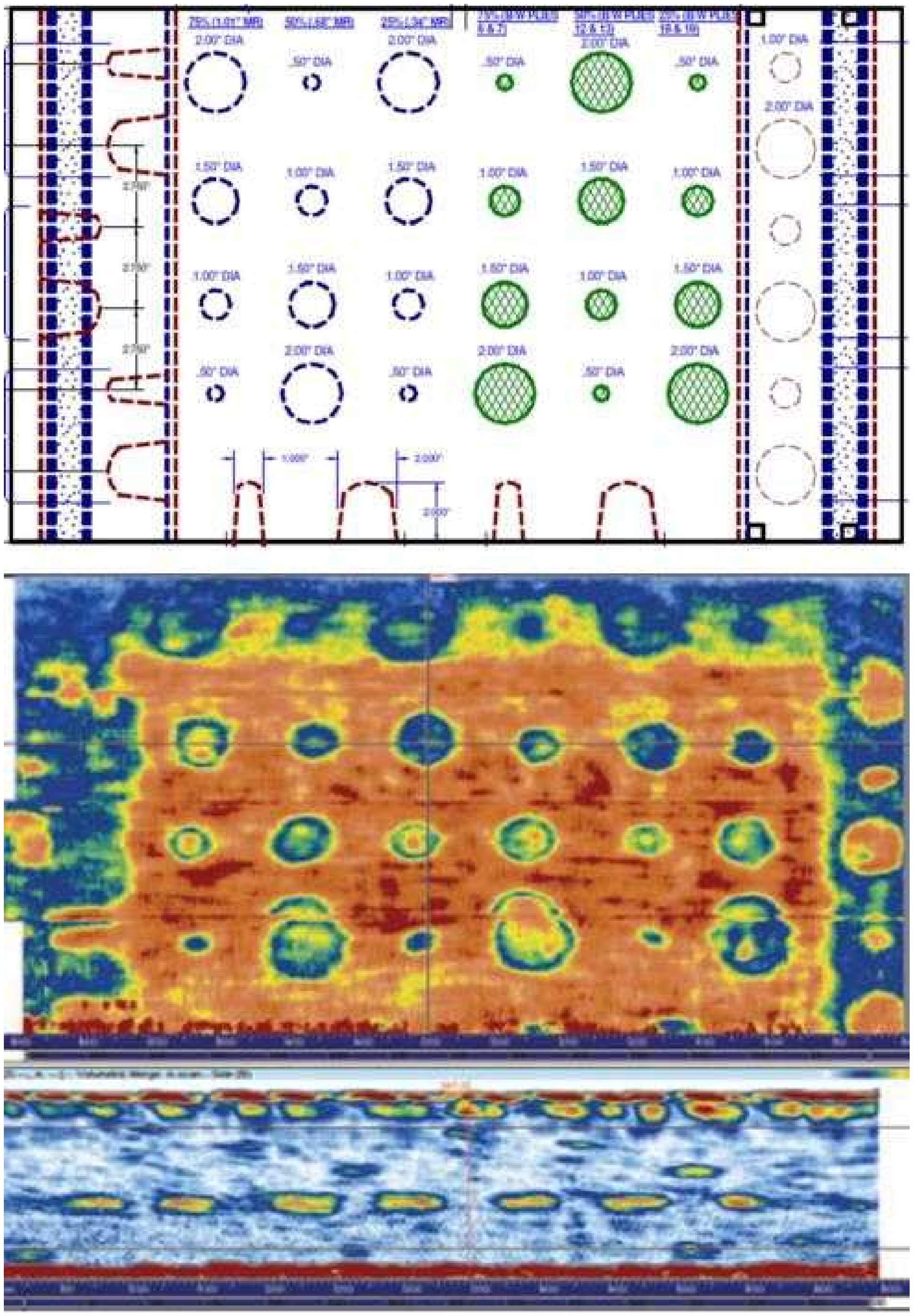

Figure 8. OmniScan PA-UT C-Scan of REF-STD-2-127-173-SNL-1
Produced by the 25 mm Water Column Shoe.

Figure 9 shows PA-UT results for specimen Wind Specimen REF-STD-7-214-265-SNL-1. This has a thick spar cap (2.14”) and thicker depth to the back of the spar-to-shear web adhesive layer (2.65”). The thickness of this specimen was deemed too thick for a 25mm water column to allow inspection of the adhesive joint so only the contact wedge was used on this sample. Insights and summary of results from the OmniScan PA-UT device deployed with the 1.5L42 probe in the contact wedge/shoe are as follows:

- Good coupling was achieved. As always with this wedge on a flat interface, the amplitude is not constant as there is some variability in element orientation relative to the surface due to uneven hand pressure on the wedge while scanning.
- The laminate is noisier than specimen 6 as evidenced from the time-of-flight C-scans. This affects defect detectability in the adhesive joint regions.
- The Amplitude and Time-of-Flight C-scan shows most of the flaws within the laminate with the exception of several mold release flaws at plies 23-31. Most of the flaws within the adhesive joint regions can also be detected with a Time-of-Flight C-scan with the appropriate color palette adjustment. This appears to be the only way to visualize the micro-balloon region at interface 1 (between adhesive joint and shear web).
- The adhesive voids in the shear web bonded joint were detected. In general, grease shows up very clearly down to a flaw size of 0.5". The microballoons can be detected regardless of where they appear within the laminate structure down to a flaw size of 1.0" and sometimes 0.5". Microballoons can be detected at the interface between the spar cap laminate and the adhesive but not on the far side of the adhesive. The pillow inserts at interface 1 do not show up in these C-scans due to the challenging noise within the laminate.
- Overall, the pillow inserts at interface 1 do not show up well on any C-scan. These flaws are however visible by scrolling through the A-scan data.

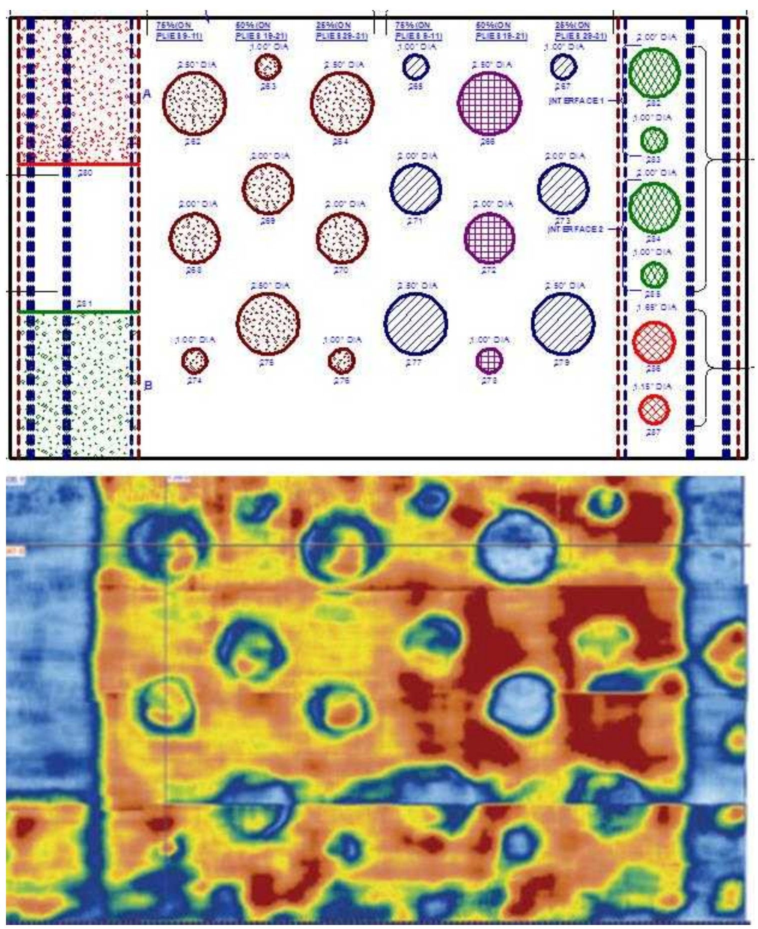

Figure 9. OmniScan PA-UT C-Scan of REF-STD-7-214-265-SNL-1 Produced by the Contact Wedge Shoe.

The Wind Specimen Adhesive Step Wedge NDI Reference Standard was used to assess an NDI method's ability to quantify the thickness of an adhesive bond line. This is important to the use of an NDI method for careful accept-reject decisions on shear-web-to spar cap bond joints. This specimen is comprised of a roughly 18 mm thick laminate with an adhesive backing having multiple thicknesses (see Figure 10). The Adhesive Step Wedge NDI Reference Standard was scanned using the 1.5L64-I4 probe and Aqualene wedge with a Glider X-Y scanner. The 25mm Aqualene delay-line was just long enough to pick up the thickest adhesive step. The thickness gate (Gate A/ in this case) was positioned just after the laminate/adhesive interface. The results in Figure 11 show that the steps are clearly visible. The color coding in the C-scan and the B-scan depth view both quantify the thickness of the adhesive layer in the bond line.

Probe and Wedge/Shoe Design - The various probe and wedge configurations each have their advantages and disadvantages. It must be recognized that these were prototypes. The results provided by this study do not show a clear indication of whether an optimal wedge design for wind blade inspections would be of a contact type or a water column type in order to inspect the entire blade. It depends on the material and the thickness of the part. The 25mm water column provides a very good inspection of the laminate (spar cap) up to a certain thickness. However, some of the samples tested would have required a very long water column to inspect the shear web which, in actual in-service conditions, can become unmanageable. In these cases, a contact approach shows some promise. One of the large aperture probes used in this study appeared to present some backing echo issues which increased the front wall dead-zone despite using a water column. Furthermore, although the results obtained with both large apertures probes were acceptable, it is conceivable that an improved probe and wedge can be defined that may be a better compromise between probe penetration power and wedge footprint. For most shear web adhesive inspections, a contact wedge would be sufficient as long as the tips of the blades are not too thin.

UT Imaging - The results presented in this report have shown that time-of-flight (TOF) C-scans are useful for imaging significant flaws within the laminate. However, the noise levels inherent in wind blades may not allow for any useful TOF representation. In all cases, gating the back wall of the laminate also works well for detecting laminate flaws. C-scan imaging of the shear web adhesion flaws is significantly more difficult due to the natural echo originating between the spar cap and the adhesive joint. For such inspections, the B-scan display seems to provide good imaging. It is possible to use up to 5 gates with the OmniScan TomoView software, however the noise level of these samples would prevent most of the useful gating synchronization techniques that could have been employed to generate multiple C-scans of the various interfaces.

The results presented herein demonstrate that PA-UT provides a feasible means for inspecting glass fiber reinforced plastic wind blades. The prototype probes and wedges used for these tests provide some of the best results obtained on this set of wind blade specimens. It appears that a complete wind blade inspection solution may require both a water wedge and a contact wedge to cover all inspection requirements.

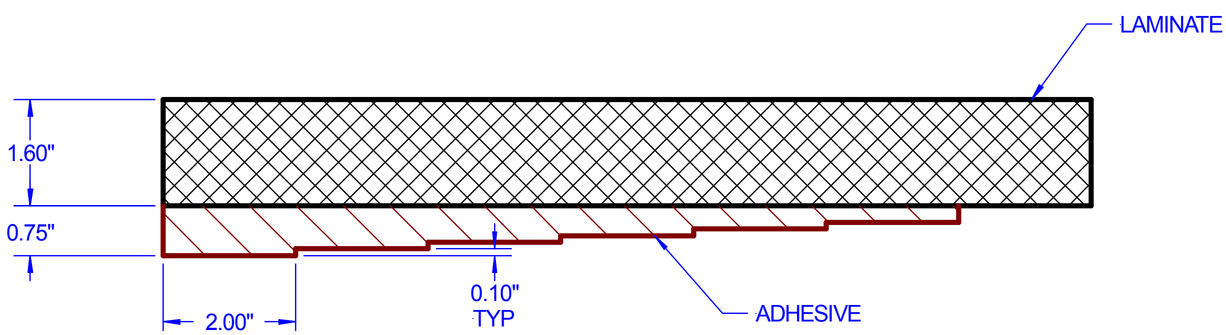

Figure 10. Adhesive Step Wedge NDI Reference Standard – Schematic.

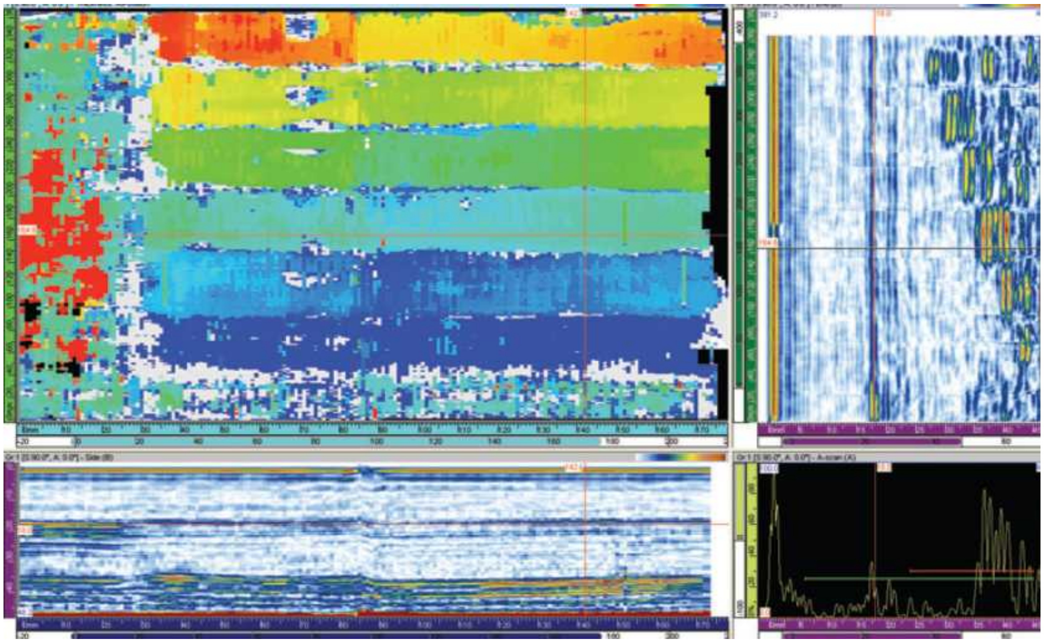

Figure 11. OmniScan PA-UT Amplitude C-Scan, B-Scan and D-Scan Images for Adhesive Step Wedge NDI Reference Standard.

In order to evaluate a different method for deploying PA-UT, the *Sonatest Linear Array WheelProbe (RapidScan 2 Device)* was applied to a series of WINDIE panels. Figure 12 shows the RapidScan along with the rolling Array WheelProbe deployed on a wind NDI test specimen. The Sonatest RapidScan 2 instrument used a modified receive amplifier with dedicated low bandwidth response for enhanced sensitivity to defect detection in attenuating composites. The low frequency WheelProbe designed for inspection of thick fiberglass composites, utilizing a 100 mm long array with 20 mm element elevation and 1MHz center frequency for optimum coupling, area coverage and penetration. Figure 13 shows the flaw profile of wind NDI test specimen REF-STD-2-127-173-SNL-1 along with labels for the set of line scans that were completed by the RapidScan 2 WheelProbe to produce the overall C-scan image of the part. Time-of-Flight information was used to arrive at depths associated with each reflection. The calibration color code used to relate indications to depth within the part is shown in Figure 14.

Figure 12. Sonatest RapidScan 2 – Linear Array UT WheelProbe Design.

The test specimen was inspected in horizontal rows where the width of the Array WheelProbe was sufficient to cover the largest 2” defects within each scan pass. Time Corrected Gain (TCG) was used but no detailed calibration was undertaken. However, the use of TCG in this investigation did help ensure equal sensitivity versus depth for equally sized defects. Amplitude and depth C-Scans were recorded and indications from the defects were then annotated with diameters in order to establish agreement with the part schematic. The scan resolution was 2 mm in both the scan and index axes. Results from the application of the 1 MHz RapidScan 2 on wind specimen REF-STD-2-127-173-SNL-1 are shown in Figure 15 and 16. Echoes were gated between the front and back wall indications, at a threshold set to minimize readings from general low level material noise typically found in thick fiberglass composites. The results are plotted in a color map with an inch scale according to the color scheme shown in Figure 14.

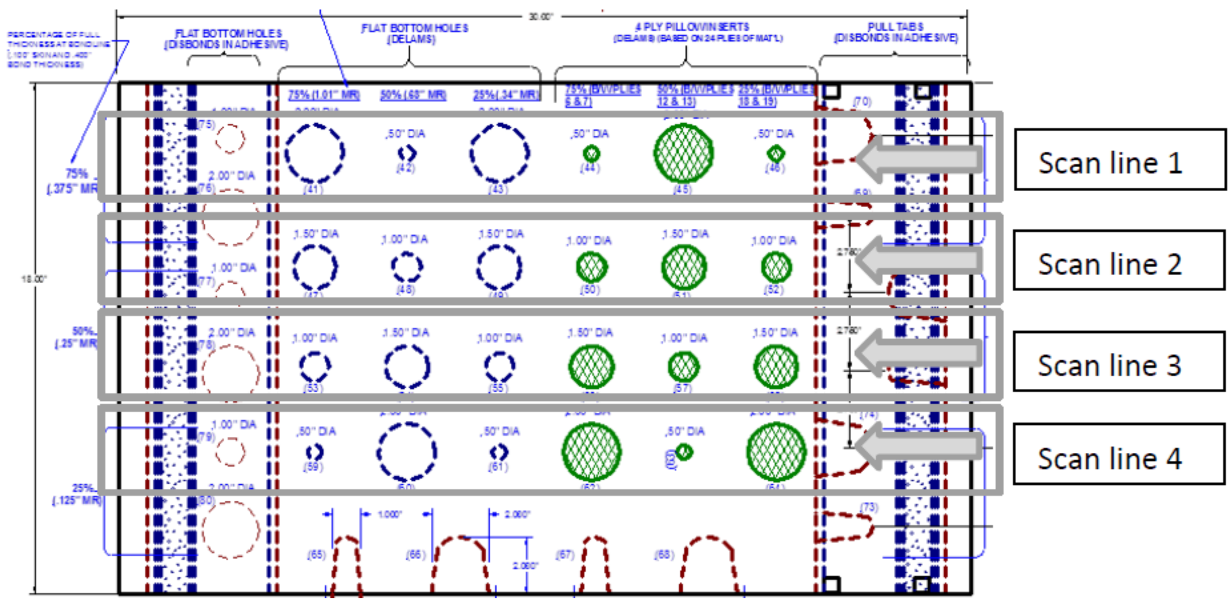

Figure 13. Flaw Schematic of Wind NDI Specimen REF-STD-2-127-173-SNL-1 Showing Series of Line Inspection Scans Used to Produce the C-Scan Image.

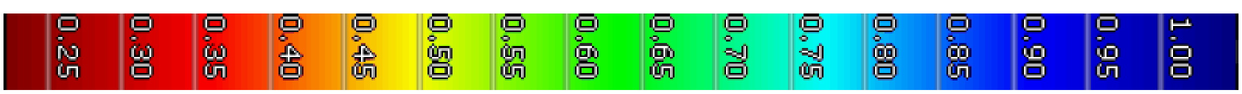

Figure 14. Calibration Color Code Used to Relate Indications to Depth Within REF-STD-2-127-173-SNL-1.

Figure 15 focuses on the spar cap laminate portion of the test specimen. It can be seen that all flaws in the spar cap, down to the smallest 0.5" diameter flaws, were successfully imaged in the C-scan. Defects were sized with the RapidScan software by drawing defect annotations (Circles, Ellipses, Lines, Rectangles, and Polygons) onto the C-Scan. They appear in all scan subsets and their positions and sizes may be judged from depth and amplitude data. Figure 16 shows a segment of results from the portion of inspections that focused on the bond line flaws. These inspections used a 500 KHz probe to detect these deeper flaws. The two sizes of flat bottom holes at each of the depths within the adhesive layer were detected. However, the pull tab flaws in the adhesive layer were not imaged in any of the scans produced by the RapidScan 2 device with the Array WheelProbe.

Overall, the RapidScan 2 instrument was used to ultrasonically inspect a fiberglass spar cap test specimen. Excellent results were achieved with 100% detection of flat bottomed holes and ply pillow inserts within the 1.27" thickness spar cap section of the sample. However, pull tabs in the adhesive layer between the spar cap and the shear web were not detected. Time Corrected Gain and Velocity parameters were estimated for the material and were used to provide flaw depth and size information with results generally within 0.1".

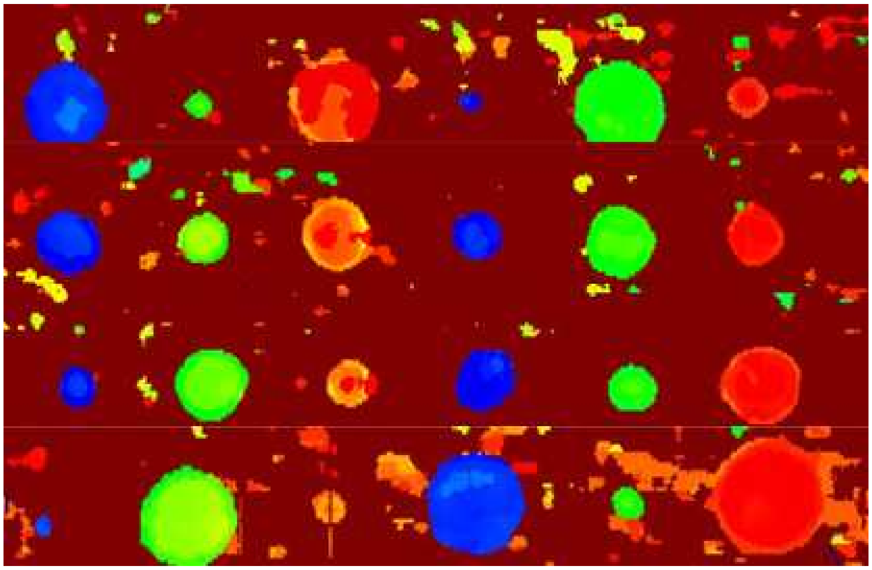

Figure 15. Linear Array UT C-Scan of REF-STD-2-127-173-SNL-1 Produced by the RapidScan 2, 1 MHz Array WheelProbe.

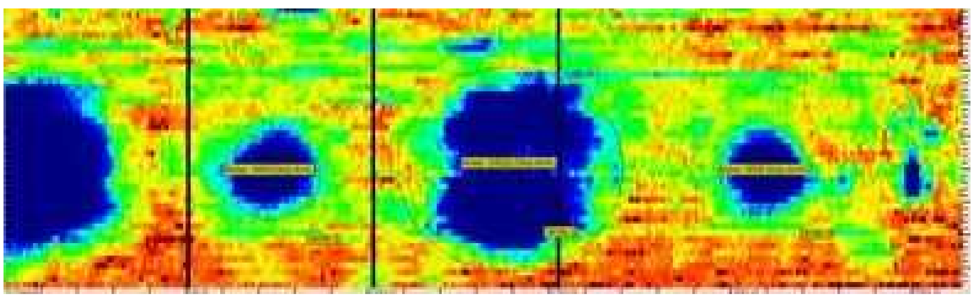

Figure 16. RapidScan 2 500 KHz Linear Array UT C-Scan of Bond Line Flaws in REF-STD-2-127-173-SNL-1.

C. Air Coupled Ultrasonics

Ultrasonic inspections traditionally involve the use of a couplant material often deployed in a continuous manner using a water pump, immersion tank or a water squirter system to properly transmit the ultrasonic wave from the transducer into the part being inspected. However, ultrasonic inspection by immersion or squirter systems cannot always be conveniently applied in the field. For these practical and operational reasons, non-contact, air-coupled ultrasonic (AC-UT) has the distinct advantage of being a couplant-free ultrasonic inspection technique. For this reason it is an attractive alternative for certain applications, even though AC-UT also suffers from several significant disadvantages, the most significant of which is the attenuation and loss of signal that accompanies air transmission of the UT signals. A summary of the AC-UT hardware and setup used in these inspections is as follows: 1) scanner with UTEX Winspect software, 2) QMI Sonda-007CX pulser/receiver, 3) QMI focused UT probes with both 120 KHz and 225 KHz frequencies.

The results from the Air Coupled UT method were respectable and show promise for wind turbine blade inspection. These methods are currently not as sensitive in detecting flaws as some of the other advanced UT methods being studied such as scanner deployed phased array, but have other advantages. Noncontact NDI methods do not require direct coupling to the surface of the part thus eliminating many deployment challenges. But air coupling the UT signal does increase attenuation and may reduce sensitivity.

All scans were made on a laboratory scanner, running UTEX Winspect software. AC-UT components consisted of the QMI Sonda-007CX pulser receiver with QMI focused probes in both 120 KHz and 225 KHz frequencies. Both AC-UT in through-transmission and one-sided pitch/catch methods were used. In many cases, the specimens were scanned in sections, with the resulting C-scans pieced together into a single image. The photos in Figure 17 show the AC-UT test set-up for both through-transmission ultrasonics (TTU) and one-sided pitch/catch mode. In AC-UT through transmission mode the transmitter is on one side and the receiver is on the opposite side of the test specimen. Thus, this approach requires access to both sides of the part in order to complete the inspection. In AC-UT one-sided pitch-catch mode both the transmitting and receiving transducers are positioned on the same side of the test specimen so inspections can be completed from a single side. This is the preferable mode of operation as access to both sides, and the corresponding ability to align the front and back transducers, cannot be guaranteed.

The AC-UT one-sided pitch/catch was evaluated where some scans involved the use of a dual density foam blocker (as shown in 17 right side) which was machined at the proper pitch/catch angles in order to eliminate the specular waves (noise). Figure 18 contains the drawing of the bond joint test specimen REF-STD-5-154-TPI-1 which contains Pillow Inserts (tight interply delaminations), microballoons (porosity) and Pull Tabs (interply delaminations). The one-sided pitch/catch method showed higher contrast in bond line variations than the TTU method. The one-sided pitch catch Amplitude C-scans offered marginally better response than the TTU and the method would be more convenient in the field as two-sided access is difficult. The OSPC approach also enabled a Time-of-flight (TOF) style gating scheme that allowed further differentiation between flaw regions. These results show that the four Pull Tabs at the edges are clearly visible along with the four Pillow Inserts and the two largest microballoon regions. Other regions of the sample produce similar low amplitude signatures which may indicate porosity in the part.

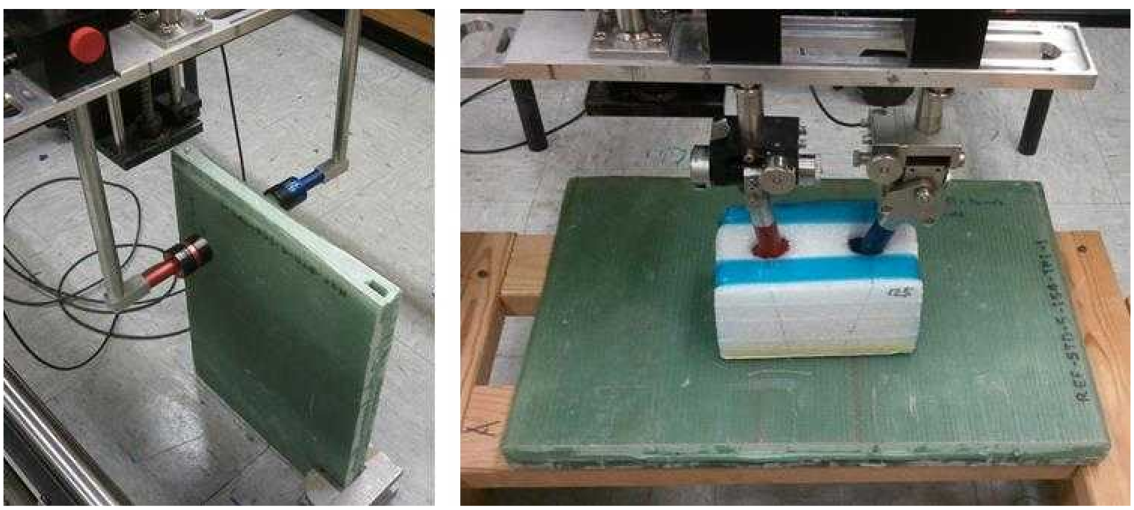

Figure 17. Air Coupled UT Applied to a Wind Blade Test Specimen in Both Through-Transmission Mode (left photo) and One-Sided Pitch/Catch Mode (right photo).

AC-UT was also applied to specimen WIND-3-110-SPAR-150 which was produced from an actual blade and contains flaws in the spar cap laminate and the bond line region. The flaw details of the test specimen are shown in Figure 19 and the resulting C-scan image generated by AC-UT TTU is shown in Figure 20. Sensitivity to defects in the spar sample was reasonable on the larger diameter flaws.

Results from the Air Coupled UT methods were fairly good and showed promise relative to wind turbine blade inspection. They currently are not as sensitive (in detecting flaws) as some of the other advanced UT methods being studied such as contact phased array UT. In order for the techniques to get to that level, further testing, development, and progress in the technology will be required. One of the major benefits of AC-UT is that it is a noncontact method. Noncontact NDI methods are not required to couple directly to a surface thus eliminating some deployment challenges. Air coupling of the UT signal does increase attenuation so this may potentially reduce sensitivity. Other factors that need to be considered for this NDI technique are set-up in a production facility, training, inspection coverage, and costs.

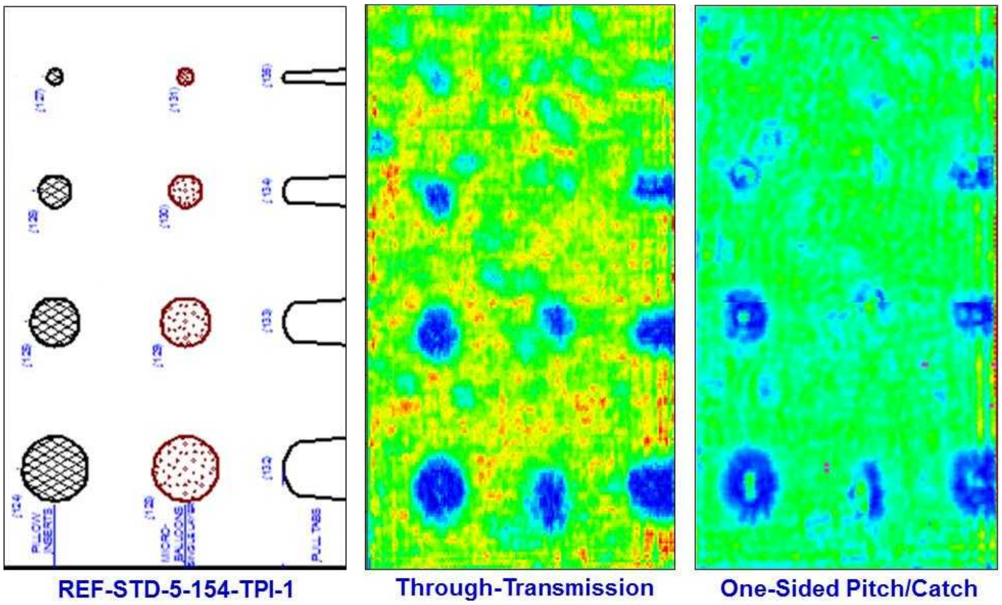

Figure 18. Air Coupled UT C-scan Comparison Between TTU and One-Sided Pitch/Catch Setup on Blade Bond Joint Test Specimen REF-STD-5-154-TPI-1.

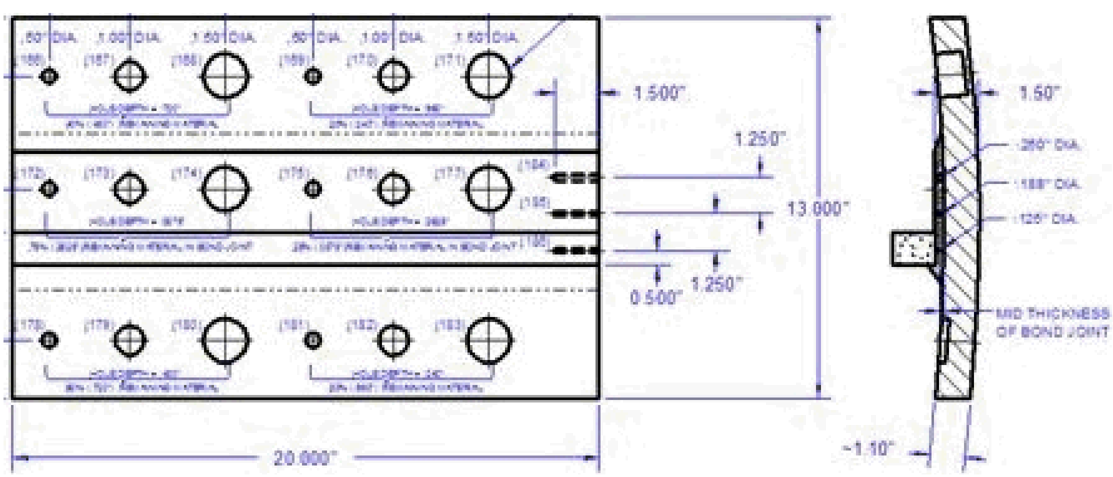

Figure 19. Dimensions and Flaw Lay-Out for NDI Specimen WIND-3-110-SPAR-150.

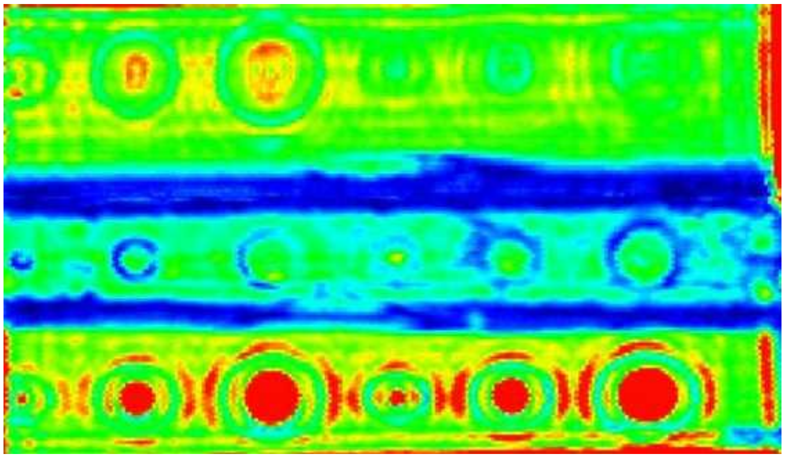

Figure 20. ACUT TTU C-scan Image Produced by 120 KHz Inspection of WIND-3-110-SPAR-150.

D. Pulsed Thermography

Initial investigations to evaluate the viability of thermography for wind blade inspections were conducted using the *Thermal Wave Imaging EchoTherm Pulsed Thermography* system. Figure 21 shows the deployment of the EchoTherm system to the set of WINDIE test specimens. Normal pulsed thermography operation uses very brief flashes of quartz lamps to produce the temperature differential (heat flow) through the part. However, in thick composite sections, such as those used in wind blades, more heat energy needs to be applied in order to observe damage corresponding to heat flow variations through the part thickness. Thus, a heat gun was used on the thick WINDIE specimens in order to induce a sufficient heat differential for detecting deeply embedded flaws.

Figure 22 shows one of the first tests for the TWI thermography system. The primary purpose was to assess the depth of penetration of the heat and the corresponding sensitivity of the IR system to detect deeply embedded flaws. It can be seen that simulated disbond/delamination flaws, represented by the flat bottom holes at the depths shown in Figure 22, were imaged down to a depth of 0.75" when heated from the front surface. It can be seen that most of the flat bottom holes are detected in the thermography images with the exception of the most challenging flaws that are located on the back side of the adhesive bond line. These flaws are further away from the inspection surface and are very close to the back wall surface making it difficult to image the very small difference in heat transfer at this depth.

Figure 21. TWI Thermography System Inspecting a Wind Blade NDI Specimen.

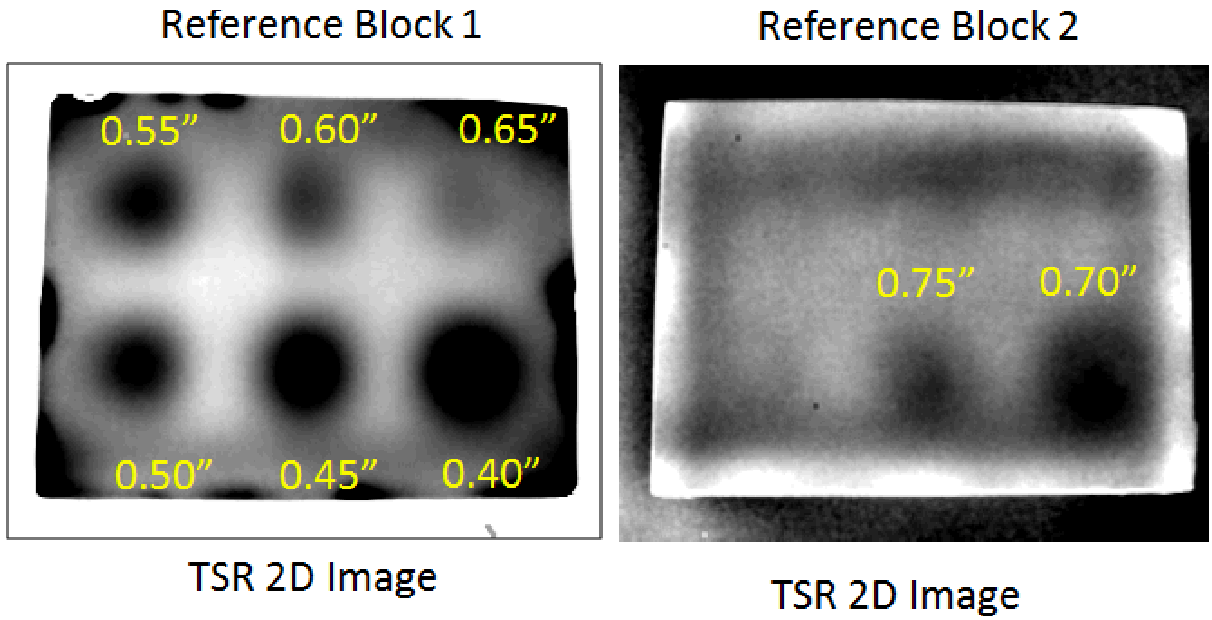

Figure 22. Thermography Images Produced by TWI IR System Applied to Wind Blade NDI Reference Standard Blocks.

Specimen REF-STD-2-127-173-SNL-1 includes a thicker spar cap (1.27” th.) and thicker adhesive joint at the spar cap-to-shear web flange interface (1.73” th.). In Figure 23, flat bottom holes in the spar cap laminate were detected at the various depths but the flat bottom holes in the bonded shear web joint were not detected. It appears that all sizes of the flat bottom holes were detected. Some pull tab flaws in the laminate at 25% depth were detected while the deeper pull tab flaws at 75% were not. None of the pull tabs in the shear web bonded joint, both at the upper and lower adhesive interface, were detected. It can be seen that almost all of the flaws, in both the spar cap laminate and shear web bond line, were detected. The only flaws that were not detected in this specimen were the pull tab disbond flaws in the adhesive bond line at Interface 1 (back side of the adhesive in the spar cap-to-shear web bond joint). Flat bottom holes in the spar cap laminate were detected at each of the depths and the flat bottom holes in the bonded shear web joint were also detected. Pull tab flaws in the laminate at all depths were detected.

Overall, these results indicate that depth of penetration is a concern for thermography inspections of wind blade specimens. Other studies [2], along with this one, have determined that IR – and in particular this TWI EchoTherm system - performs well for wide area imaging to detect near surface flaws and performs well on sandwich core areas. Substructure flaws must manifest themselves as changes (anomalies) in the surface temperature of the part in order to be detected by thermography. Small flaws, especially those embedded deep within a structure, are difficult to image as their presence has less of an effect on surface temperature heat transfer. Thermography also works very well for NDI of sandwich construction. As a result, this method should be considered for any needs with respect to wide-area inspection of foam or balsa core regions, including post-repair inspections in the field.

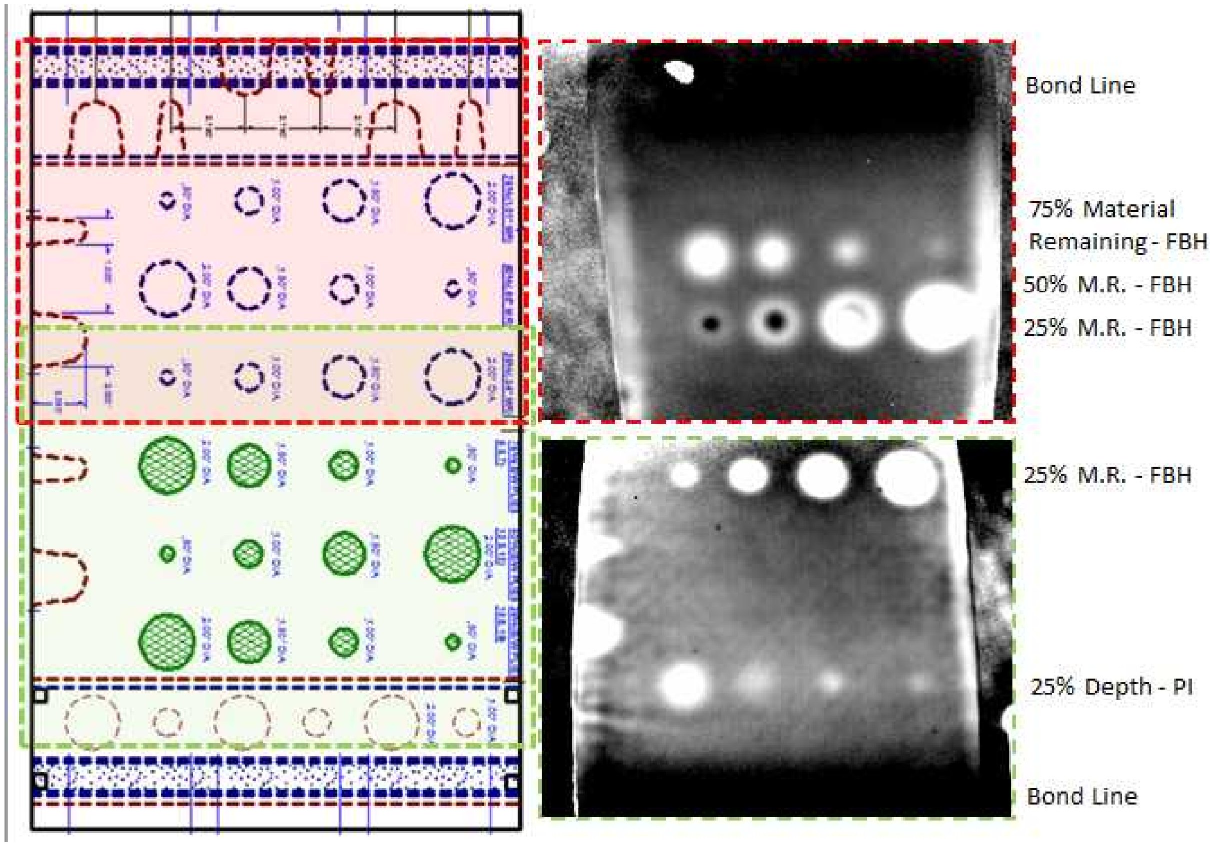

Figure 23. Thermography Images Produced by TWI IR System Applied to NDI Specimen REF-STD-2-127-173-SNL-1 Containing Spar Cap and Shear Web Bond Line Flaws.

E. Comparison of NDI Methods

One sample was selected to show how direct comparisons of NDI methods can be made and to demonstrate how WINDIE inspection results can be used to develop, evaluate and validate the array of potential NDI methods for flaw detection in wind turbine blade structure. Many different inspection techniques were evaluated in the WINDIE experiment. For the purpose of this overview comparison exercise, several methods were selected and the results are compared below.

The sample selected for inter-comparison of the methods discussed here was REF-STD-4-135-SNL-1. This particular sample contained a 1.45" thick spar cap and included two types of flaws. They were dry areas and out-of-plane waves. The out-of-plane waves were created by embedding pre-cured resin rods with a specific aspect ratio (width to height) between plies of the laminate prior to resin infusion. Figure 24 shows the schematic of the sample used to display the results from the ten selected NDI methods. Following is a summary of some results from this common inspection challenge to show just some of the NDI method comparison aspects of this program. Additional review of the full suite of NDI test specimens contained in the WINDIE NDI screening study is necessary to draw final conclusions regarding the viability of each NDI method for detecting any of the flaw types found on wind blades.

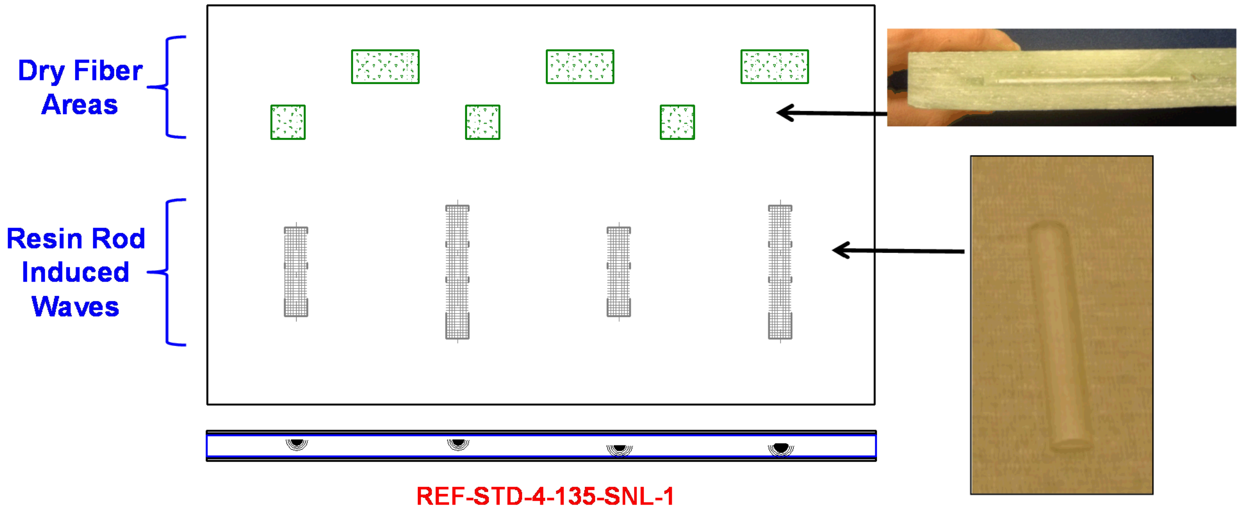

Figure 24. NDI Feedback Specimen REF-STD-4-135-SNL-1 with Out-of-Plane Waves and Dry Fiber Regions.

GE Global Research NDI Method: Microwave - Figure 25 shows that this inspection method was able to detect 8 flaws out of 10 in the WINDIE specimen containing out-of-plane waves and dry regions. The sensitivity level of microwave radar depends of several factors including power of the transmitter, frequency range and directional selectivity of the antenna. All of the flaws in the spar cap sample were detected with the exception of two dry areas. These particular dry areas require the deepest penetration, at 75% depth of laminate.

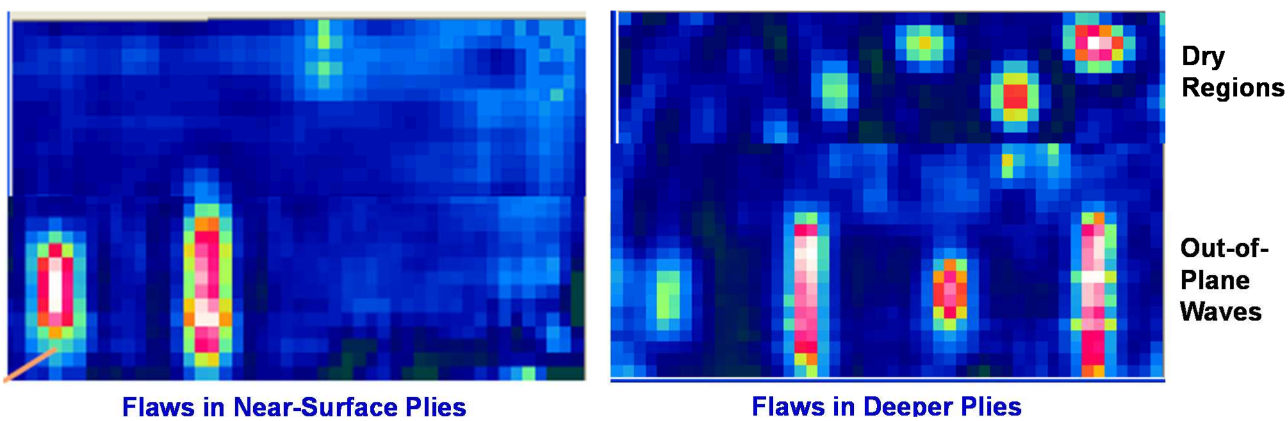

Figure 25. GE Microwave Inspection Results from Fiberglass Specimen REF-STD-4-135-SNL-1.

Iowa State University NDI Method: Air Coupled Ultrasonics - Air Coupled UT was deployed in one-sided pitch/catch mode as this is the most feasible approach for use on wind blades. Specimen REF-STD-4-TPI-1 was inspected using the one-sided pitch/catch Air Coupled UT method with the resulting C-scan images shown in Figure 26. The one-sided pitch catch approach also enabled a Time-of-flight (TOF) style gating scheme that allowed further differentiation between flaw regions and clearly identified all defects in specimen REF-STD-4-TPI-1. The ability to apply TOF gating methods can significantly increase sensitivity.

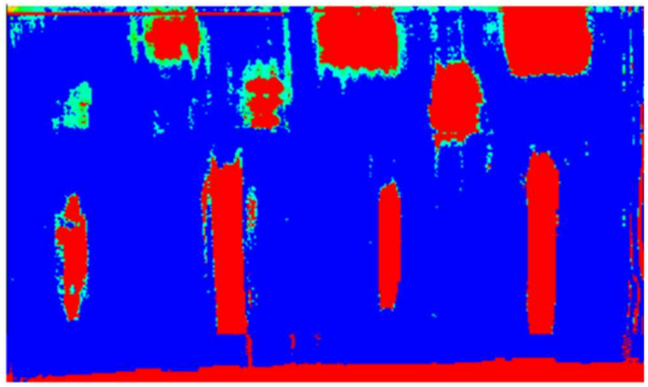

Figure 26. Air Coupled Ultrasonic Inspection of Fiberglass Specimen REF-STD-4-135-SNL-1 and C-Scan Results Showing Detection Capabilities.

Olympus NDT NDI Method: Phased Array Ultrasonic - As shown in Figure 27, all out-of-plane waves and dry areas were detected using phased array UT. All flaws show up quite clearly with the amplitude C-scans. All resin starved flaws are detected. Interply waves are detected clearly by their effect on the back wall signal. Near surface flaws (less than 5 mm deep) in thick laminates tend to be more difficult to detect using low frequency ultrasonic techniques due to the dead zone of the probe and high noise levels created at the water path to fiberglass interface. Use of a delay line, in this case the 25 mm water column shoe, avoids this inspection impediment and allows for the detection of near-side flaws.

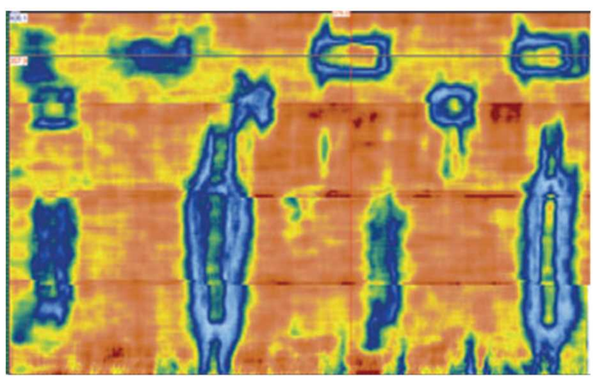

Figure 27. OmniScan Phased Array Ultrasonics Inspection of Fiberglass Specimen REF-STD-4-135-SNL-1 and C-Scan Results Showing Detection Capabilities.

The exercise presented above demonstrates some basic comparison steps that are used to complete the evaluation of NDI methods for wind blade inspections. Overall, the results from the WINDIE testing provided an extensive database to properly screen NDI methods for wind industry applications. It should be noted that all inspections were conducted with the inspector having full knowledge of the flaw types and flaw profile in each test specimen. Thus, the tests were not conducted in a blind fashion, rather in "feedback" mode where experimenters could adjust, modify and optimize their equipment to show its maximum capability. That is why this effort is referred to as an NDI screening study. The results sited here can be used to select the best and most promising NDI methods to potentially address particular inspection requirements. This study allowed for an overall assessment of technology maturity along with some preliminary evaluation of NDI sensitivity, deployment, flexibility and inspection speed. The performance of the top NDI methods are now being quantified in a statistically-valid Probability of Flaw Detection (POD) experiment which will involve both advanced NDI and conventional NDI as deployed by wind industry inspectors. The wind POD study, which is the follow-on to the WINDIE NDI screening effort discussed in this paper, will use inspections on flawed wind blade parts to: 1) establish the industry baseline POD for flaw detection capabilities using existing wind blade inspection practices, and 2) quantify the degree of inspection improvements that can be achieved via the use of advanced NDI methods. All inspections will be conducted in a blind mode where the inspectors do not know the specimen flaw profiles. NDI deployment, to maximize throughput in the factory, and human factors issues will also be studied in this forthcoming POD experiment.

A thorough inter-comparison of the set of results obtained from the WINDIE prorgam was completed in order to arrive at a set of ratings for each NDI method studied. Table 2 compares the ratings that were determined through the WINDIE experiment. The ratings are broken down into the various inspection regions and depth of penetration demands. This rating system classifies the NDI methods into multiple categories ranging from excellent (optimum - sensitive and universally suitable) to good (promising - could be evolved into a functioning tool) to limited (works only on select regions of the wind blade) to poor (not a candidate NDI method for wind blade inspections).

Note the far right-hand column in Table 2. It provides a rating for the Technology Readiness Level (TRL) associated with each NDI method. One analysis of the advanced NDI results assessed the maturity of each inspection technique based on the observations from the WINDIE Experiment. Standard Technology Readiness Levels (TRL), which are similar across DOE, DOT, NASA and DOD, were used to place each inspection method into an appropriate TRL category. Table 3 describes each of the TRL levels ranging from basic concepts (TRL 2) to fully functional and tested/marketed technology (TRL 9). Table 2 shows that most of the NDI methods were deemed to be in the latter or final stages of development and ready for utilization. It was observed that some of the devices could benefit from customization to address the unique demands of thick composite laminate inspections.

Suitable Inspection Areas for Inspecion Techniques							
Method	Spar Cap	Spar Cap to Shear Web Bond Line	Leading & Trailing Edge	Sandwich Structure	Deep Subsurface Flaws	Near Surface Flaws	Technology Readiness Level (TRL)
Microwave	Good	Satisfactory	Limited	Good	Good	Good	7-8
Shearography	Satisfactory	Poor	Limited	Excellent	Insufficient	Good	9
Terahertz Radiation	*	*	Excellent	Excellent	*	*	7
Oblique Incident Ultrasonics	Good	Good	*	*	*	*	8-9
Pulse Echo Ultrasonics	Excellent	Excellent	Satisfactory	Insufficient	Excellent	Good	9
Phased/Linear Array Ultrasonics	Excellent	Excellent	Satisfactory	Insufficient	Excellent	Good	9
Air Coupled Ultrasonics	Good	Good	Good	Good	Good	Good	7-8
Pulsed Thermography	Limited	Poor	Limited	Excellent	Insufficient	Good	9
Lock-In Thermography	Limited	Poor	Limited	Excellent	Insufficient	Good	7-8
Millimeter Wave	*	*	*	Good	*	*	5-6
* Determination cannot be made due to the lack of specimens inspected by this particular method							

Table 2. Sample Summary of Results from NDI Methods Applied to WINDIE Experiment.

It can be seen that the phased/linear array ultrasonic methods along with the focused pulse-echo ultrasonic methods were deemed to be the most universally-suitable for wind blade inspections. The exception to this relates to the inspection of foam, balsa or other core sandwich construction. Inspection of composite sandwich structures, while dealt with in a limited manner in the WINDIE program, was not thoroughly studied. Inspection of composite sandwich structures will be evaluated further in future NDI studies, especially those that address the inspection of wind blade repairs.

For the solid laminate inspections emphasized in the WINDIE program, a set of promising NDI methods were identified. These are methods that may be less mature than phased/linear array ultrasonic methods or focused pulse-echo ultrasonic methods but that demonstrated good inspection sensitivity in both thick and thin laminates and bonded joints. These methods include air-coupled ultrasonics, terahertz radiation and microwave NDI techniques. Additional development in these NDI methods could improve their sensitivity to provide an alternative to contact ultrasonic-based NDI methods.

Due to the physics of how they work, several of the NDI methods demonstrated that, while limited on depth-of-penetration, they work well in detecting near-surface flaws. These techniques include thermography and shearography. The wide area nature of these methods also produces the ability to inspect large regions quickly. These near-surface oriented inspections also work well on the sandwich construction test specimen which has a thin laminate skin. The successful application of thermography and shearography for inspecting composite honeycomb structures was also clearly determined in other, related studies [2].

Technology Readiness Levels for the Department of Energy	
Technology Readiness Level	**Description**
TRL 1.	Scientific research begins translation to applied R&D - Lowest level of technology readiness. Scientific research begins to be translated into applied research and development. Examples might include paper studies of a technology's basic properties.
TRL 2.	Invention begins - Once basic principles are observed, practical applications can be invented. Applications are speculative and there may be no proof or detailed analysis to support the assumptions. Examples are limited to analytic studies.
TRL 3.	Active R&D is initiated - Active research and development is initiated. This includes analytical studies and laboratory studies to physically validate analytical predictions of separate elements of the technology. Examples include components that are not yet integrated or representative.
TRL 4.	Basic technological components are integrated - Basic technological components are integrated to establish that the pieces will work together.
TRL 5.	Fidelity of breadboard technology improves significantly - The basic technological components are integrated with reasonably realistic supporting elements so it can be tested in a simulated environment. Examples include "high fidelity" laboratory integration of components.
TRL 6.	Model/prototype is tested in relevant environment - Representative model or prototype system, which is well beyond that of TRL 5, is tested in a relevant environment. Represents a major step up in a technology's demonstrated readiness. Examples include testing a prototype in a high-fidelity laboratory environment or in simulated operational environment.
TRL 7.	Prototype near or at planned operational system - Represents a major step up from TRL 6, requiring demonstration of an actual system prototype in an operational environment.
TRL 8.	Technology is proven to work - Actual technology completed and qualified through test and demonstration.
TRL 9.	Actual application of technology is in its final form - Technology proven through successful operations.

Table 3. Description of Technology Readiness Levels.

One final NDI method comparison is provided in Table 4. This table lists the basic NDI categories and summarizes the strengths and limitations of each major NDI method. All NDI methods present some set of strengths and inspection limitations. The inspection requirements and desired performance levels (e.g. sensitivity, versatility, inspection rate) will determine which NDI method is optimum for each application.

III. Conclusions

The intention of this study was to determine which Nondestructive Inspection (NDI) technologies are most promising for wind turbine blade inspections, assess those technologies, and transfer the technology to industry through inspection procedure development and inspector training. Through the WINDIE study, conducted under the Sandia Labs Blade Reliability Collaborative, various NDI technologies were assessed on a set of standardized wind turbine blade test specimens that contained engineered defects. Based on these results, phased array ultrasonics (PA-UT) was selected for further development and introduction at blade manufacturing facilities. Hardware was developed and customized to optimize UT sensitivity and deployment to address blade inspection needs. Inspection procedures were developed and beta tested at blade production facilities. Both laboratory and field tests were conducted to study this NDI technology and to ensure that all deployment issues were properly addressed. In addition to flaw and damage detection, customized pulse-echo UT can provide diagnostic information regarding bond line thickness and porosity levels in the assembly. This study has identified one best overall NDI method while determining complimentary NDI methods that can be applied to produce a comprehensive blade inspection system. The detection of fabrication defects helps enhance plant reliability and increase blade life. Improved inspection of operating blades can result in efficient blade maintenance, facilitate repairs before critical damage levels are reached and minimize turbine downtime while increasing blade operation lifetimes.

NDI Technique	Deployment Options	Inspection Limitations	Inspection Strengths
Ultrasound	Single Element, Through Transmission, Focused Immersion, Air-Coupled, Phased Array (PA), Linear PA, Focused PA, Laser, Acoustic Video, High Frequency Bond Test (Resonance)	Sound Attenuation, coupling for contact testing	Depth of penetration, high resolution, many deployment options (hand held or scanning)
Thermography	Pulsed, Lock-In, Vibro, Sonic, Scanning Line, Induction	Depth of penetration, long soak times and data acquisition time required for thicker material	Large area for each image, non-contact
Radiation	X-Ray, Terahertz (between IR and microwave)	X-Ray radiation hazards	High resolution, limited deployment options, non-contact
Microwave	Gantry and scanning systems	Maturity of technology, gantry/scanner deployment required	Non-contact
Millimeter Wave	Gantry and scanning systems (Gigahertz range)	Maturity of technology, gantry/scanner deployment required	Non-contact
Shearography	Varying methods to stress the test article such as heat, pressure and mechanical vibration	Thickness/stiffness, sensitive to part movement	Wide area, limited set up required, wave detection capabilities, non-contact

Table 4. Summary of General Capabilities for the Major NDI Categories Applicable to Wind Turbine Blade Inspections.

References

1 Roach, D., Neidigk, S., Rice, T., Duvall, R., Paquette, J., "Blade Reliability Collaborative: Development and Evaluation of Nondestructive Inspection Methods for Wind Turbine Blades," Sandia DOT Report, SAND2014-16965, September 2014.

2 Roach, D., "An Inspector Calls - The Search for Hidden Flaws in Composite Honeycomb Structures," *Journal of Aerospace Testing International*, Vol. 24, No. 6, 2004, pp. 40-47.

Acknowledgments

Sandia National Laboratories is a multi-program laboratory managed and operated by Sandia Corporation, a wholly owned subsidiary of Lockheed Martin Corporation, for the U.S. Department of Energy's National Nuclear Security Administration under contract DE-AC04-94AL85000.